

# Optical Pumping of $Rb^{85}$ and $Rb^{87}$

Herbert D. Ludowieg

May 10, 2017

## Abstract

Optical Pumping is a spectroscopical method that was developed in the 1950's and has been a very accurate method to determine spectroscopical properties of certain materials. In this experiment the following were determined: the individual g-factors, nuclear spins, cross sectional area and ratio of the periods. For  $Rb^{85}$  the g-factor and nuclear spin were found to be:  $0.3260 \pm 0.0005$  and  $2.571$  respectively. For  $Rb^{87}$  they were found to be:  $0.482 \pm 0.001$  and  $1.576$  respectively. The cross-sectional area and ratio of the periods were found to be:  $1.8 \times 10^{-16} \pm 0.3 \times 10^{-16}$  and  $1.44 \pm 0.05$  respectively.

## I. Introduction

Optical Pumping is a spectroscopical method developed in 1950 by Alfred Kastler, whom received the Nobel Prize in physics in 1966 for his discovery. This method is one in which photons are utilized to create population differences of electronic excited and ground states. So the meaning and general concept is in the name itself.

Under standard conditions the population difference required to carry out experiments is not possible because from statistical mechanics at thermal equilibrium we have an equal number of electrons that rise and fall from excitation levels. Due to this, they tend to cancel each others effects and no net population differences can be detected. This is also the basis of lasers where, a population difference needs to be created so that photons can be spontaneously emitted by the lasing medium.

For this experiment the equipment that is being used is provided by TeachSpin and consists of an Radio Frequency (RF) discharge lamp, Interference Filter, Polarizers, Quarter Wave plate, absorption cell, optical detector, three sets of magnetic coils in a Helmholtz configuration and a RF magnetic coil. The sample is a rubidium glass bulb that contains neon gas with a pressure of approximately 0.04 atm pressure. The presence of the neon gas is important as its spherical symmetry will reduce the interactions between the rubidium atoms and the outside environment. They will act as a buffer gas.

Optical Pumping is a process in which has had much applicability in solid state and liquid state physics. However, we will only be dealing with a gas since at the solid and liquid phases the interactions between the neighboring atoms increases thus broadening the energy levels [1].

## II. Theory

### (i) Structure of alkali atoms

In the experiment described in this paper we will be studying the absorption and emission from rubidium isotopes (85 and 87) which are alkali atoms. As such the electronic structure of rubidium is as such,

$$1s^2 2s^2 2p^6 3s^2 3p^6 3d^1 4s^2 4p^6 5s$$

Where we can show the shorthand version as,

$$[Kr]5s$$



Figure 3: *Coupling of angular momentum in an electron [3].*

Where, the superscripts show the number of electrons contained in each of the electronic shells. Since the only valence electron is in the 5s shell we can consider the atom to be consisting of only one electron. This electron much like with other electrons can be described by means of the total angular momentum of the electron  $\vec{J}$  where it is made up of components  $\vec{S}$  and  $\vec{L}$ . Which, represent the spin angular momentum and orbital angular momentum respectively. The vectors are shown on figure 3

Since, these components are vectors we can represent the total angular momentum as such,

$$\vec{J} = \vec{S} + \vec{L} \quad (1)$$

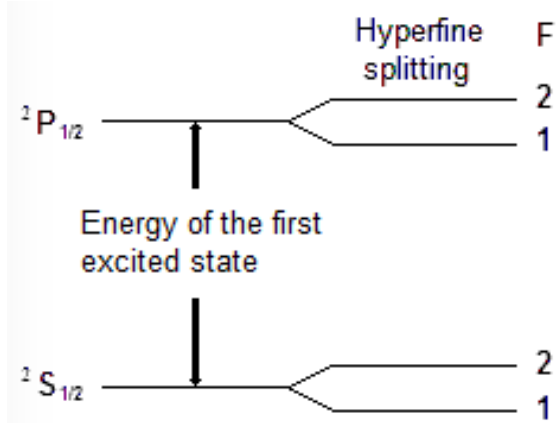


Figure 1: *Hyperfine splitting energy diagram for  $I = 3/2$  particle [3]*

Where, for an alkali atom in the ground state the value of  $\vec{L}$  is zero from the quantum numbers associated with the orbital shell and the value of  $\vec{S}$  will be  $1/2$ . So, this gives rise to a total angular momentum of  $1/2$ .

As it will later become apparent, we will display some of the energy levels in the notation  $^{2s+1}L_J$ . Where, all of the values are those taken from equation 1. To represent the ground state of an alkali atom we can write it with the formatting  $^2S_{1/2}$ . Since the value of  $\vec{L}$  is zero by convention we write it as the letter S. Where it to be 1 we would write in P and so on.

If the electron were to be in a P state it would be able to have an angular momentum of  $\vec{L} \pm \vec{S}$  and would take on the representations  $^2P_{1/2}$  and  $^2P_{3/2}$ . Due to the difference in angular momentum the energy levels would have different energies. This arises due to the spin-orbit coupling of the angular momentum vectors [4].

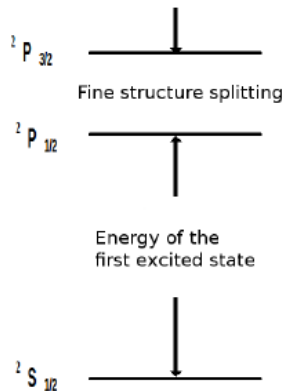


Figure 4: *Pictorial representation of the energy difference in the fine structure. Not to scale [3].*

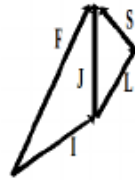


Figure 2: *Hyperfine coupling in an alkali atom [3]*

So far, we have been ignoring the effects of the nucleus to make the theory easier. However, this will not go on any longer. We will now consider the hyperfine splitting of the electron angular momenta. This arises from the spin-spin coupling where for the fine structure we had the spin-orbit coupling. The spin-spin coupling is due to the magnetic dipole moment of both the proton and electron. Now, it should be noted, that the magnetic dipole moment of the proton is much smaller than that compared to the electron. The dipole momenta can be given as the following.

$$\vec{\mu}_p = \frac{g_p e}{2m_p} \vec{S}_p \quad \vec{\mu}_e = -\frac{e}{m_e} \vec{S}_e [4] \quad (2)$$

Where, the p and e represent the proton and electron values respectively,  $g_p$  and  $g_e$  are the respective g-factors of value 5.59 and 2.00 and  $\vec{S}$  represents the respective angular spin. Using derivations outlined in reference [4] we can get to an expression for the difference in energy of the two states with different angular momenta. The equation is as such.

$$\Delta E = \frac{4g_p \hbar}{3m_p m_e^2 c^2 r^4} [4] \quad (3)$$

Where, c is the speed of light and r is the radius of the atom. In the reference they are making an example to a hydrogen atom with r equal to a (Bohr's atomic radius). This derivation can still be generalized to our use as we are dealing with an atom that can be approximated to be one that is like a hydrogen atom, due to the closed nature of the inner shells. Where we can also make the relation with the frequency as such.

$$\nu = \frac{\Delta E}{h} [4] \quad (4)$$

Where the Hamiltonian is as such.

$$H = h\vec{I} \cdot \vec{J} [3] \quad (5)$$

Usually the energy difference between these two levels is very small and one can cause transitions in the hyperfine structure with an RF wave. A pictorial representation of the coupling of the magnetic dipole moment spins is shown on figure 2. Where a rough energy separation schematic is given in figure 1. As is clearly seen the energy that is required to jump from one energy level to the next is much greater than that required to make the transition in the hyperfine structure. Later we will discuss the implications of this with respect to optical pumping.

However next we will show another form of splitting where all of the degenerate energy levels of the electronic energy level diagram are split.

## (ii) Interaction of an alkali atom with a magnetic field

This interaction is better known as the Zeeman effect and the general premise behind this effect is that by applying a magnetic field to an atom we can further split the degenerate energy levels according to their angular momenta.

In the Zeeman effect there are three main regions that are to be considered: weak field, intermediate and Strong field effects. For the purposes of this experiment we will only deal with the weak field effect as the strong field can require magnetic fields around 10T which is only achievable with extremely expensive equipment.

The Zeeman effect is an effect which can break the spin-orbit coupling of an electron creating a difference in energy between the different orbitals of an atom. The weak field Zeeman effect is named as such because the energy splitting from the Zeeman effect is very small comparatively and as such the Hyperfine splittings dominate with the Zeeman effect becoming the perturbation [4]. The hamiltonian of this effect is as shown.

$$H = h\vec{I} \cdot \vec{J} - \frac{\mu_J}{J} \vec{J} \cdot \vec{B} - \frac{\mu_I}{I} \vec{I} \cdot \vec{B} [3] \quad (6)$$

Where,  $\mu_J$  is the electronic dipole moment and  $\mu_I$  is the nuclear magnetic dipole moment.

Figure 5 shows the energy levels from the weak field Zeeman effect. The energy levels are splitting into  $2F + 1$  levels. Where F is the angular momentum of the atom, M is the projection of F onto the direction of the magnetic field. In figure 3 we show two levels for the ground state and the first excited

state. For this experiment we are only considering the first excited state  $^2P_{1/2}$ . The reason why we only consider this and not the  $^2P_{3/2}$  is because at  $\vec{J}$  values of 1/2 we can calculate the energy levels in closed form from quantum mechanics with the Breit-Rabi equation.

Since the electron can be considered to be a moving charge with charge  $1.6e-19$  Coulombs. This magnetic dipole moment has a value that is equal to the Bohr Magnetron,  $\mu_B$ . Ignoring the effects of the nucleus we can then represent the magnetic energy as [3].

$$U = \frac{M(\vec{L} + 2\vec{S}) \cdot \vec{J}}{J^2} \mu_B B = g_J \mu_B M B [3] \quad (7)$$

Where,  $g_J$  is the Lande g-factor which describes the change in the magnetic moment of an electron bound in an atom, B is the magnetic field and M is the atomic spin component along the magnetic field direction. The g-factor is given by,

$$g_J = \frac{(\vec{L} + 2\vec{S}) \cdot \vec{J}}{J^2} \quad (8)$$

$$g_J = 1 + \frac{J(J+1) + S(S+1) - L(L+1)}{2J(J+1)} [3]$$

To show the interaction energy of an electron we simply need to add a negative sign to equation 7 from the negative charge of the electron. In the case of rubidium where we have a J and S value of 1/2 we find that the g-factor is equal to 2.00232 [3].

Now, if we were to include the interaction of the nucleus to find the interaction energy the equation could be represented as follows.

$$U = -g_F \mu_B M B [3] \quad (9)$$

Where,  $g_F$  can be shown to be the following.

$$g_F = g_J \frac{F(F+1) + J(J+1) - I(I-1)}{2F(F+1)} [3] \quad (10)$$

Where, F represents the total angular momentum of the atom, I is the total nuclear spin angular momentum and J is the total electronic angular momentum. This quantity is highly dependent on the atom that is being used and as such there is no one set value as with the Lande g-factor.

We can then show the transition frequency as.

$$\nu = \frac{g_F \mu_B B}{h} [3] \quad (11)$$

The above equations are only applicable when the interaction energy with the magnetic field is very

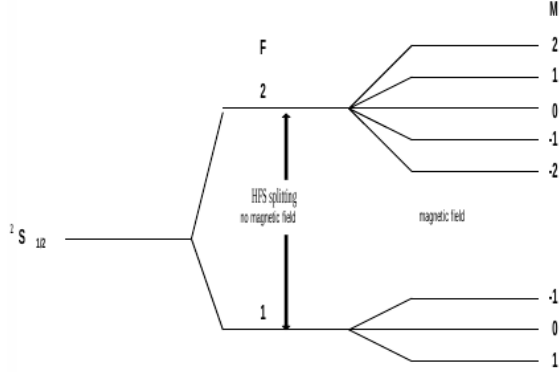


Figure 5: *Energy levels of an alkali atom of the  $2S_{1/2}$  state in a weak magnetic field [3]*

small and depends linearly. If the dependence is quadratic, which will be studied in this experiment, we must apply the Breit-Rabi equation which can be derived by diagonalizing the Hamiltonian in equation 6 [3]. The result of such is the following.

$$W(F, M) = -\frac{\Delta W}{2(2I + 1)} - \frac{\mu_I}{I} MB \pm \dots \quad (12)$$

$$\frac{\Delta W}{2} \left[ 1 + \frac{4M}{2I + 1} x + x^2 \right]^{1/2} [3]$$

Where,

$$x = (g_J - g_I) \frac{\mu_B B}{\Delta W} [3] \quad (13)$$

$$g_I = -\frac{\mu_I}{I\mu_B} [3] \quad (14)$$

Where,  $W$  is the interaction energy and  $\Delta W$  is the hyperfine splitting energy.

Figure 7 shows a plot of the Breit-Rabi equation. The three Zeeman levels for the magnetic field are as follows. Weak field is at an  $x$  value close to zero where the energy splitting varies linearly and the hyperfine interaction dominates where the Zeeman effect is the perturbation. The strong field region, also known as the Paschen-Back region is  $x$  values greater than 2 where the energy levels are linear once again and depends on the Zeeman effect where the hyperfine splitting is taken as the perturbation. The final region is the intermediate field region at values greater than zero but less than 2. In this region both the hyperfine splitting and the Zeeman effect contribute equally to the energy splitting of the electronic orbitals [4].

In this experiment we are only concerned with the weak field Zeeman effect.

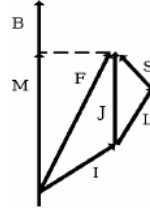


Figure 6: *Zeeman effect in an alkali atom [3]*

### (iii) Photon absorption in an alkali atom

The lowest electronic state along with the first two excited states of the valence electron for a rubidium atom are the following:  $2S_{1/2}$ ,  $2P_{1/2}$  and  $2P_{3/2}$ . Where, we will mainly deal with the ground state and the first excited state for simplicity.

The transitions from the ground state to the excited state are governed by selection rules that are as follows:  $\Delta L = 0, \pm 1$ ,  $\Delta S = 0$  and  $\Delta J = 0, \pm 1$ . However, the value of  $L$  cannot go from 0 to 0 [3]. For this experiment we are interested in the amount of light that is absorbed or transmitted by the rubidium atoms in a given volume. For this purpose it can be useful to use the concept of a cross section of the atoms. In the limit of low density this can be represented as.

$$n = n_0 e^{-\sigma \rho l} [3] \quad (15)$$

Where,  $n$  and  $n_0$  are the incoming and outgoing flux of electrons and  $\rho$  is the density of the gas.

A similar concept can be employed when talking about a flux of photons.

$$I = I_0 e^{-\sigma_0 \rho l} [3] \quad (16)$$

Where the cross section in this equation is actually the cross section at the resonance condition which is much lower than the expected value.

Now we must append to our selection rules for transitions to account for the selection rules for the hyperfine splitting which will add that  $\Delta F = 0, \pm 1$ . Additional splitting caused by the magnetic field adds that  $\Delta M = 0, \pm 1$ .

The selection rule for  $M$  can be somewhat different, because since angular momentum must always be conserved the photons that are absorbed must

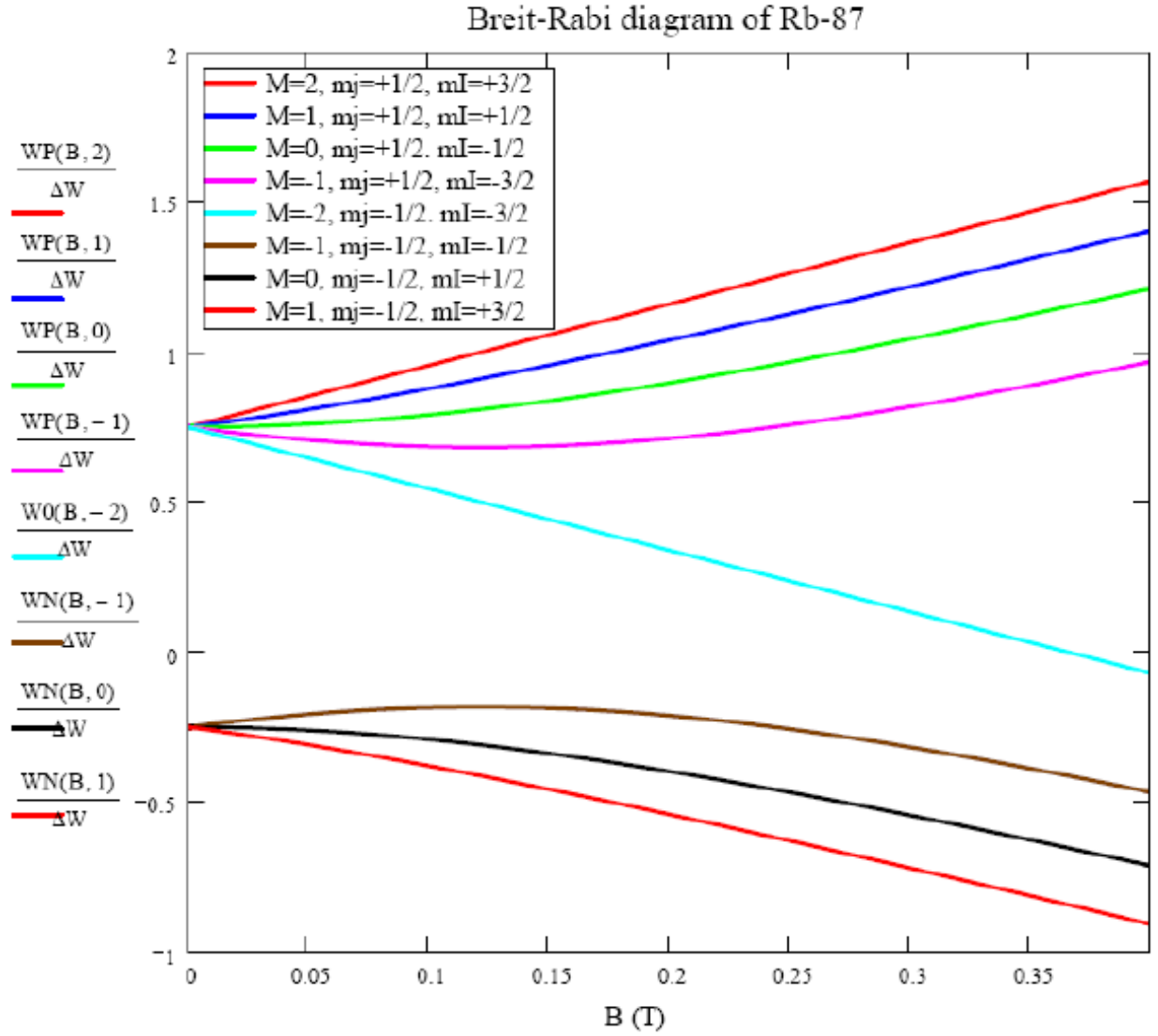


Figure 7: Breit-Rabi diagram of  $\text{Rb}^{87}$  in a magnetic field [3].

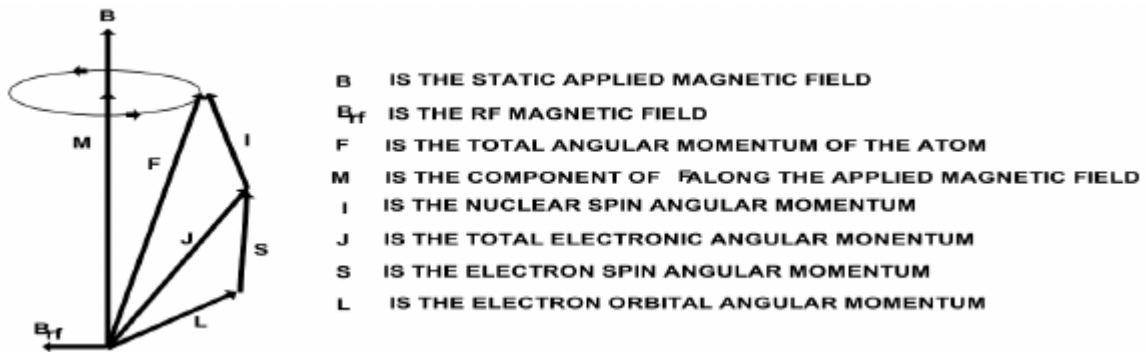


Figure 8: Magnetic fields and angular momenta involved in the experiment [3].

be circularly polarized. Of course, if light is circularly polarized we will be adding to the angular momentum. The question then becomes how does it change depending on the polarization.

It has already been established that only circularly polarized will change the angular momentum of the atom. So, depending on the polarization we will get addition or subtraction to the angular momentum. That is to say that we will have either a +1 or a -1 to the angular momentum, never both.

The lifetime of the transitions will be determined by collision processes. It is mentioned that the rubidium glass bulb is filled with a buffer gas that is there to decrease the collisions of the atoms with the walls of the container and lose its angular momentum. The neon gas disallows this from happening and since it is a very symmetric atom it will not contribute much to the decrease of the angular momentum of the atom [1].

#### (iv) Optical pumping in rubidium

In optical pumping we are trying to create a net population difference in one state relative to another. From statistical mechanics we know that electronic states can settle into a thermal equilibrium where there is no net population difference on one state. By making use of the hyperfine splitting and the Zeeman effect along with some clever applications of the incoming photons we can achieve this.

On figure 10 we see the types of transitions that are possible. On the left side of the figure we see that there is a large separation between the energy levels that corresponds to a transition energy of a 795 nm photon. Then there are smaller gaps that come from the hyperfine splitting and then the Zeeman levels.

In order to create this 795 nm photon an RF discharge lamp is used to create circularly polarized light at that wavelength. The RF discharge lamp along with a general schematic of the experiment is shown on figure 9. Inside the RF discharge there is some  $Rb^{87}$  gas along with some metal. When a current is passed through the gas it induces a transition to populate the first two excited states. By spontaneous emission it then emits two photons, one at 795 nm and one at 780 nm. We are only interested in the 795 nm line and can filter the 780 nm line by the interference filter [3].

There is also a linear polarizer that serves a very important purpose. Previously it was shown that the M levels can be increased by using circularly polarized light. Meaning, we are not interested in the

effects of the linearly polarized light on the transitions. Why is it important that we do this you may ask. The reason is because the  $^2P_{1/2}$  state has the highest angular momentum when it has a value of  $M = 2$ . There is no  $M = 3$  state meaning that once the electrons make the transition to the  $M = 2$  state they will accumulate on that level until they can relax back to their ground configuration. By this method we create a population difference.

One should always be note that the Zeeman effect causes transitions within the atomic orbitals where the circularly polarized light causes the transitions between the different energy levels. Should also mention that this is not restricted to the positive values since it depends on the polarization direction of the light.

#### (v) Zero field transition

Before going further to talk about RF induced transitions we should mention the transitions that occur at values of zero magnetic field. The fundamental reason this happens is because the atoms are still being irradiated with the photons at the energy to excite the electrons. When the magnetic field is zero there are no effects from the hyperfine splitting or the Zeeman effect so there is, ideally, only two energy levels and have a completely degenerate system. Where, it becomes simple to populate one of them. This results in the lineshape that is shown on figure 11.

This can be used to tune the magnetic field of the apparatus and cancel off most if not all of the outside sources of magnetic fields. The equipment is extremely sensitive to tiny changes in magnetic field where a laptop being on or off can make a difference in the accuracy of the data.

One of the most prominent sources of outside magnetic field is the field that is produced by the Earth and must be cancelled by using a combination of the vertical, horizontal coils and lateral positioning of the apparatus.

#### (vi) Transient effects

Throughout this report we have been considering the optical pumping to happen only when the RF has been constantly on. Now we will consider the case when the RF signal is turned off and on at a certain frequency.

When we are at resonance the Larmor frequency for the weak field Zeeman effect is given by.

$$\omega_0 = 2\pi\nu_0 = g_F \frac{\mu_B}{\hbar} B_0 [3] \quad (17)$$

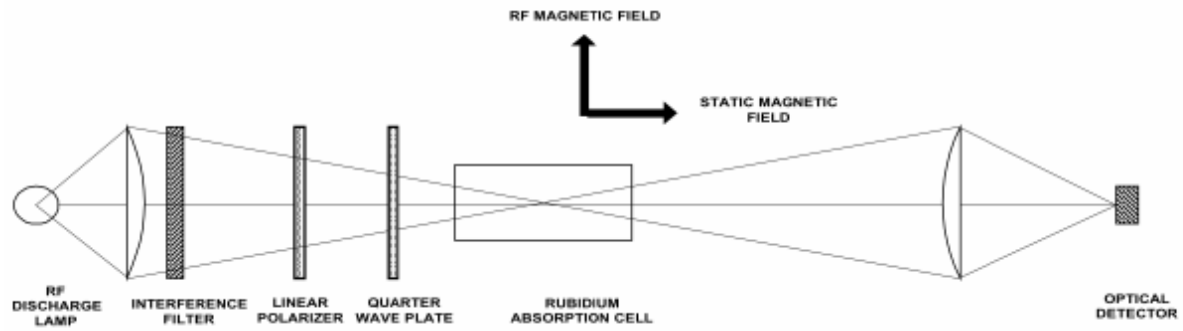


Figure 9: *Magnetic fields and angular momenta involved in the experiment [3].*

### ENERGY LEVELS FOR $\text{Rb}^{87}$ ( $I = 3/2$ ) IN AN APPLIED MAGNETIC FIELD

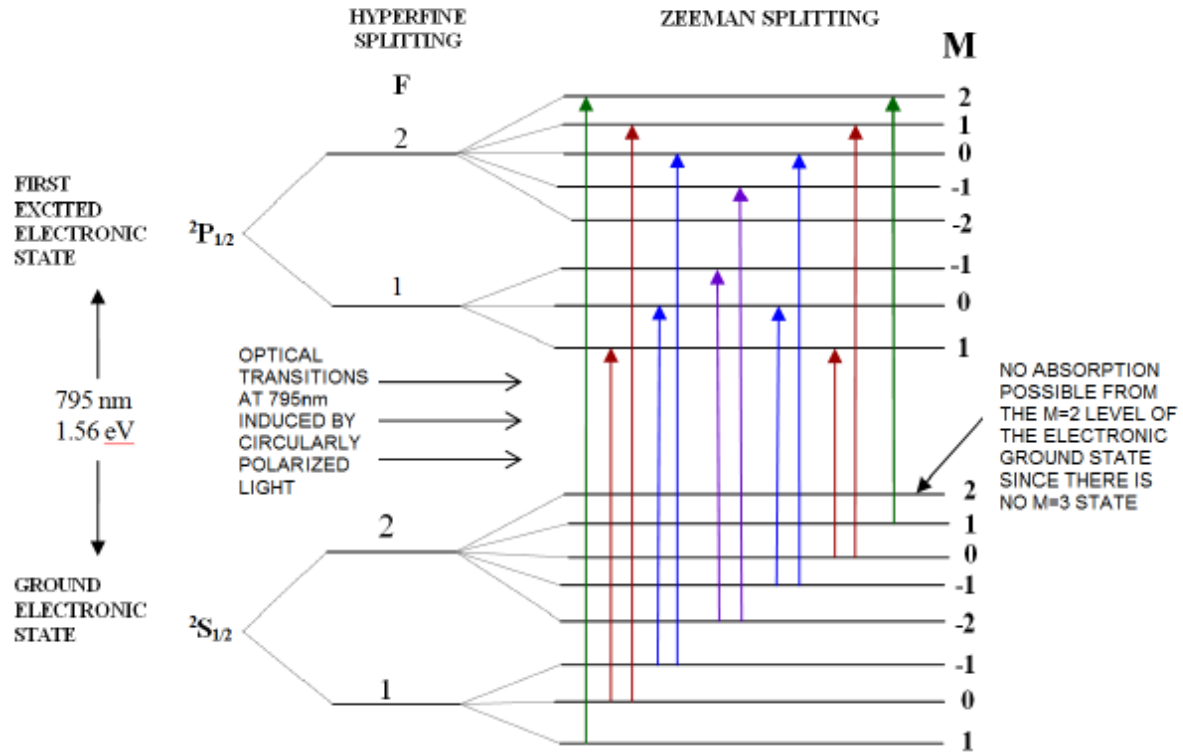


Figure 10: *Transitions involved in the optical pumping of  $\text{Rb}^{87}$  [3].*

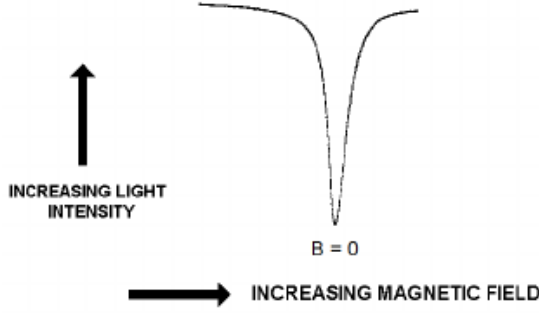


Figure 11: Zero field transition with no RF field [3].

Where,  $\nu_0$  is given by equation 11 and  $g_F$  by equation 10. We can then define the gyromagnetic ratio,  $\gamma$ , as.

$$\gamma = g_F \frac{\mu_B}{\hbar} [3] \quad (18)$$

We can then write the Larmor frequency as.

$$\omega_0 = \gamma B_0 [3] \quad (19)$$

The equations above are very similar to those employed in Nuclear Magnetic Resonance.

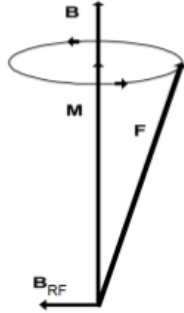


Figure 13:  $F$  vector and the precession about the magnetic field with perpendicular field  $B_{RF}$  [3].

Figure 13 shows how the total atomic angular momentum precesses about the magnetic field,  $B$ , when a perpendicular field tuned to the Larmor frequency,  $B_{RF}$ .

### III. Experimental Set-Up

For this experiment we are using a TeachSpin set-up that provides us access to the equipment that is necessary to be able to carry out the experiment without much difficulty or needing to set-up very complicated equipment.

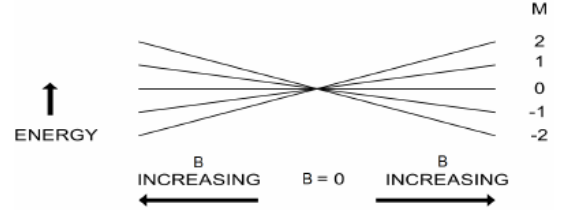


Figure 12: Energy levels near zero field with no RF field [3].

#### (i) Rubidium Discharge Lamp

The rubidium discharge lamp consists of an RF oscillator, oven and gas bulb. In the bulb there is a mixture of gas containing rubidium gas and a buffer gas. The buffer gas in the bulb is xenon. The remaining gas is a mixture of  $Rb^{85}$  and  $Rb^{87}$  with concentrations of about 36% and 64% respectively. The oven is set to a temperature of  $115^\circ \text{C}$ . The lamp takes 10 to 20 minutes in order to fully turn on and be able to equalize the temperature inside the gas bulb. It should be noted that the rubidium atoms emit light at the 795 nm range which is in the near infrared. One may be able to see some light coming from the lamp, but this light may be due to the xenon spectral line or higher lines of rubidium [3].

We are only interested in the 795 nm range line.

#### (ii) Detector

The detector is a PDB-C108 silicon photodiode from Photonic Detectors Inc. [3] With an active area of 0.25 inches in diameter and a spectral response in the 795 nm range of 0.6 A/W. Figure 14 gives a general schematic of the photodiode with some of the connections. The preamp is a current-to-voltage converter with three gain settings selectable by a switch on the detector itself.

The photodiode preamplifier has a voltage range of 0.0 V to 11.5 V and it should be kept in mind to avoid saturating the signal.

Gain Resistor (M $\Omega$ ) $\pm$ 5%	Low pass 3dB point (kHz) $\pm$ 10%	Noise ( $\mu V_{pp}$ )
1	12.0	20
3	8.0	40
10	5.0	100

Table 1: Photodiode preamplifier specifications [3]. The signal from the preamp is on a coaxial BNC



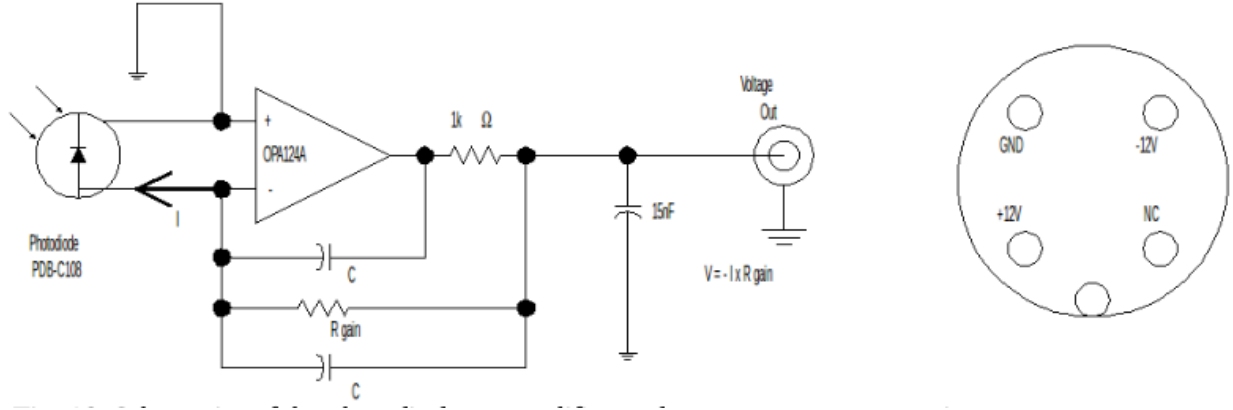


Figure 14: General Schematic of the photodiode detector with preamplifier and preamp power connections [3].

connector labeled Detector that feeds into the main housing for the analysis. This can be used to connect the cable directly to an oscilloscope and see what is being read.

The electronics houses the following sections that can help to adjust the signal from the detector [3].

- DC offset: 0-10 V DC Set by a ten turn potentiometer and fine control adjustment 0-20 mV set by a one turn potentiometer. At low gain settings the fine adjustment knob will not be very useful due to the scaling difference.
- Gain: 1,2,5 ... 100 Adjustable gain knob that will increase the signal gain. The maximum value is 1000.
- Low Pass filter: A two pole low pass filter with time constants: min., 1 ms, 10 ms, 100 ms, 1 s, 3s. When the min. value is selected, the frequency response is determined by the gain setting of the preamplifier.
- Meter: Displays the voltage reading from the detector output. The range is from -4 to +4 V with a multiplier toggle switch to increase to a range of -8 to +8 V.

### (iii) Optics

In this section we will go into the optics that are used for this experiment. The optics that will be discussed are: plano-convex lenses, interference filter, polarizers, quarter wavelength plate.

- Two plano-convex lenses: Diameter 50 mm, focal length 50 mm.
- Interference filter: Diameter 50 mm. This filter is chosen since it has the ability to absorb

the 780 nm line that is emitted and still transmit the 795 nm line that is of interest in the experiment.

- Two linear polarizers on rotatable mounts: Diameter 50 mm. The linear polarizer will be used to filter out other polarizations of light so that they can be converted into circularly polarized light with the help of a quarter wavelength plate.
- Quarter wavelength plate on rotatable mount: Diameter 50 mm, "optical thickness"  $205 \pm 5$  nm. When properly oriented, the plate can convert linearly polarized light into circularly polarized light. The plate has different optical axes which have different indices of refraction that will slow down the light beam. To produce circularly polarized light, place the quarter wave plate at a  $45^\circ$  angle to the linear polarizer.

Figure 15 gives the retardation about the different axial tilt. Tuning the optical thickness (retardation) can be accomplished by rotating the plates.

- Alignment: Throughout the experiment the optics may need to be aligned to be able to get the best results from the equipment. One way to do this is to maximize the signal gotten from the detector by moving the lenses until the signal reaches a maximum value. In theory this should work since the light incident to the lenses should be made to be linearly aligned and then re-focus into the detector to get the signal reading. If we do not get a maximum value there are two things that can be happening. The light that is coming from the lamp is

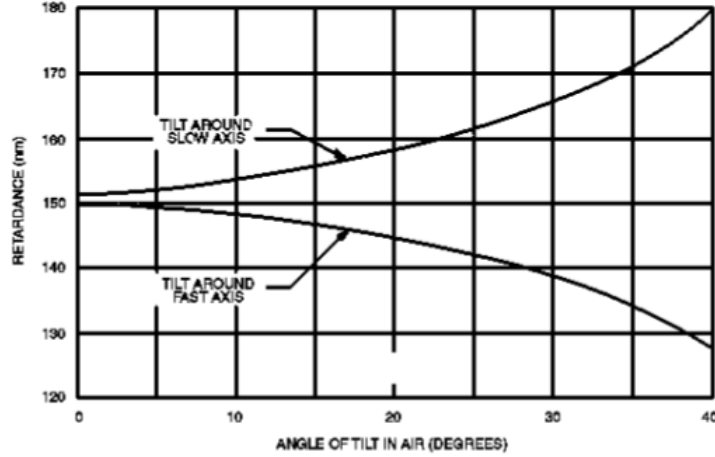


Figure 15: *Tilt tuning of the quarter wavelength plate [3].*

not being spread into a parallel beam correctly or the light that is going into the detector is not being refocused properly.

We shall look at the first problem. One possible way to troubleshoot the problem is to use a sheet of whitepaper and place it in front of the lens. Remember that the light that we are able to see with the slight purple color is the light that may be due to transitions in the xenon gas or higher energy excitations in the rubidium atoms. So, we cannot do this after the interference filter as we will not be able to see the light beam nor properly adjust the lens position. By moving the paper back and forth one should be able to see that the beam of light does not change in size which we will see as a circle. If it does diverge slightly change the lens position until it does not diverge anymore and the circle is at its maximum diameter.

Now we shall look at the second problem which will be at the detector. For this we can place the quarter wave plate and the linear polarizer in front of the discharge lamp. Due to the fact that the entire apparatus is bolted onto the rail and table we will not be able to use the same troubleshooting method as we did before, since we cannot see the light beam. What we must do is to read a signal either on the oscilloscope or a voltmeter and maximize the signal. To do this change the position of the lens on the rail and assuming that the first lens was set to its correct position the second should be in the correct position when the signal from the detector is at a maximum. This is because, the light beam that incident on the lens is supposedly parallel and constant so the lens should

refocus the light back into a single point and this point should be at the detector.

It is important to check the height of the optics which should be set to a height of approximately 3.5 inches.

#### (iv) Temperature regulation

The following components make up the cell temperature regulation system [3].

- a). Temperature regulator: Proportional, Integral, Derivative (PID) temperature controller with associated electronics. The settings for the PID are preset in the electronics box and cannot be change without changing the inner electronics.
- b). Temperature probe: Type T (Copper - Constantan) Thermocouple ( $5\text{ }\mu\text{m}$  wire). Constantan is magnetic, however, the wire was chosen to be so small so that the effect of its magnetic field on the magnetic field in the sample can be neglected.
- c). Oven: The oven consists of the following components.
  - 1). Rubidium cell: Glass bulb that contains the rubidium sample that is to be studied in the experiment.
  - 2). Cell holder: A foam insert that holds the sample.
  - 3). Heater: The heater is an open-ended glass heater that is wrapped with non-magnetic bifilar wound heater wire. The resistance is measured to be  $50\text{ }\Omega$ .

4). Insulation: Foam layer surrounding the heater.

5). Oven casing: A Plexiglass cylinder. Has endcaps of 50 mm optical windows. Holes in the casing allow wires to be run into the oven.

d). Operation: On the front face of the electronics box there is a controller window with three buttons that control the menu up and down respectively. To set a temperature one must press the menu button and cycle to SP (Set Point) and using the up and down buttons one can set the desired temperature in centigrade. To view the current temperature one can press the menu button again and press it again to show the PRC on the display. By leaving it on this setting it will display the measured temperature.

Do note that setting the temperature takes a very long time (20-30 minutes). So, the first thing that should be done when starting the lab should be to set the temperature and allow it to settle.

The minimum temperature is ambient room temperature where the max is approximately 100<sup>0</sup> C.

## (v) Magnetic Fields

All the DC magnetic fields are produced by magnetic coils that are placed in a Helmholtz configuration. There are three magnetic coils whose specs are known.

	Mean Radius (cm)	Turns/Side
Vertical Field	11.735	20
Horizontal Field	15.79	154
Sweep field	16.39	11

Table 2: Mean Radius and turns given values for the coils [3].

	Field/Amp ( $T \times 10^{-4}/A$ )	Max Field ( $T \times 10^{-4}$ )
Vertical Field	1.5	1.5
Horizontal Field	8.8	22.0
Sweep field	0.60	0.60

Table 3: Field/Amp and Maximum field specs for the coils. The Field/Amp specs are approximate [3].

## IV. Results and Discussion

### (i) Absorption of *Rb* resonance radiation by atomic *Rb*

For this part of the experiment we are trying to make an approximate measurement of the cross sectional area of atomic rubidium. The method we used to do so was by irradiating the sample with photons and measuring the intensity of the light as a function of temperature. A general schematic is outlined on figure 16. The schematic shows us that we should only have the two convex-plano lenses and the interference filter to make the measurements.

The data that was taken is given in the following table.

Temperature ( <sup>0</sup> C)	Intensity (V)
27.0	10.727
37.0	8.819
47.0	6.875
57.0	4.473
67.0	2.602
77.0	1.496
87.0	1.035
97.0	0.866

Table 4: Data taken for part i of the experiment. We then fitted the data with an exponential curve that would follow the form of equation 16, except with an added error term. The equation that was fitted using Python was.

$$Y = Ae^{-k(x-2e16)} + B \quad (20)$$

Where, k is given as the product of the cross sectional area times the path length, x is the density of the rubidium atoms which was given in the following table and y are the measured intensity values from the data.

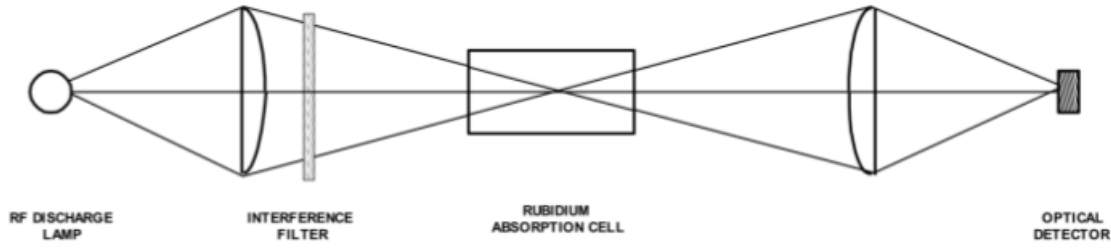


Figure 16: General schematic of the set-up for part i [3].

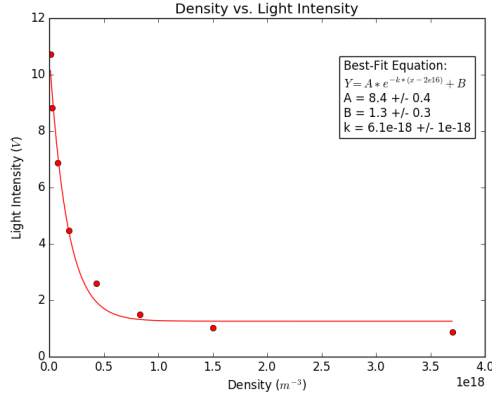


Figure 17: Light intensity as a function of density of rubidium atoms at given temperature values.

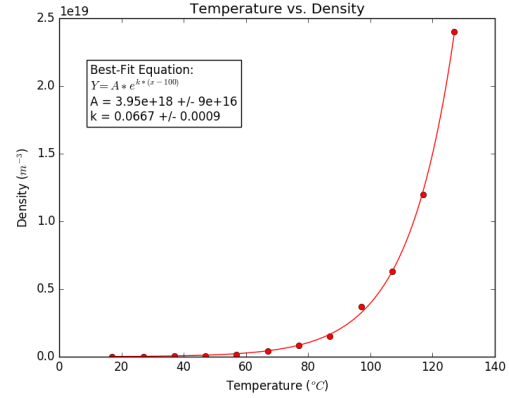


Figure 18: Density of rubidium atoms as a function of temperature.

Temperature (°C)	Density (m <sup>-3</sup> )
17	$3.3 \times 10^{15}$
27	$1.1 \times 10^{16}$
37	$2.9 \times 10^{16}$
47	$7.5 \times 10^{17}$
57	$1.8 \times 10^{17}$
67	$4.3 \times 10^{17}$
77	$8.3 \times 10^{17}$
87	$1.5 \times 10^{18}$
97	$3.7 \times 10^{18}$
107	$6.3 \times 10^{18}$
117	$1.2 \times 10^{19}$
127	$2.4 \times 10^{19}$

Table 5: Density of rubidium atoms as a function of temperature [3].

Using all of the values and the curve fitting functions in Python the cross sectional area was found to be:  $1.8 \times 10^{-16} \pm 0.3 \times 10^{-16} \text{ m}^2$ . The data was plotted on figure 17.

We also plotted the data that is given on table 5 and fitted an exponential curve to the data using Python. The results are shown on figure 18.

A quick note on the fitting functions. The values

that are subtracting from x were chosen to be those because we needed to shift the entire curve and they gave the lowest uncertainty values comparatively. The B term in equation 20 is an error term that accounts for outside sources of light that are not eliminated by the apparatus.

## (ii) Low field resonances

For this part of the experiment we began using the magnetic fields to be able to create the weak field Zeeman effect and hyperfine splitting. The general set-up for this part is given on figure 19. We then found the magnetic fields as a function of current using the equation.

$$B = \frac{8\mu_0 NI}{R\sqrt{125}} [3] \quad (21)$$

Where,  $\mu_0$  is the permeability constant, N and R are the turns and mean radius values that are given in table 2 and 3 and I was varied. During the experiment we measure the voltage value that is running through the coils but on the electrical box we can see the resistances that are given for each of the coils and by Ohm's law can calculate the current.

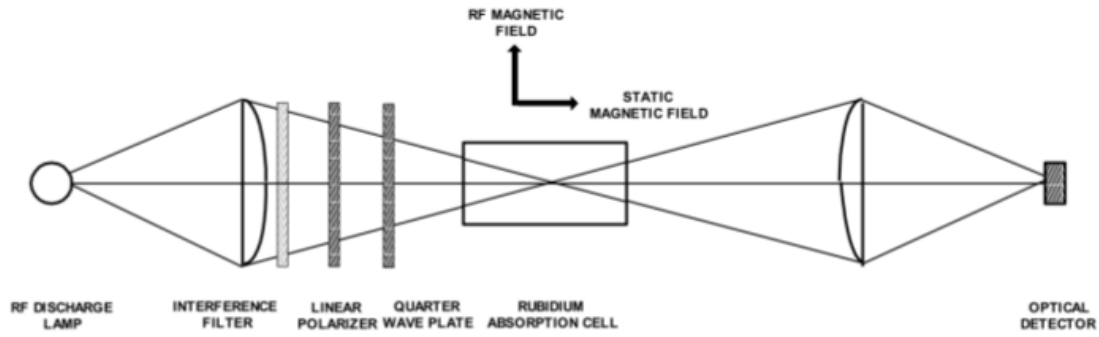


Figure 19: General schematic for part ii of the experiment [3].

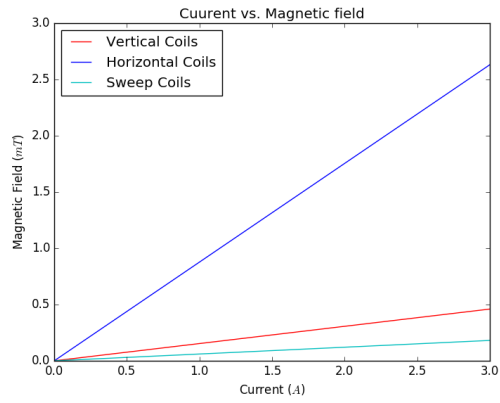


Figure 20: Magnetic field as a function of current for the three magnetic coils.

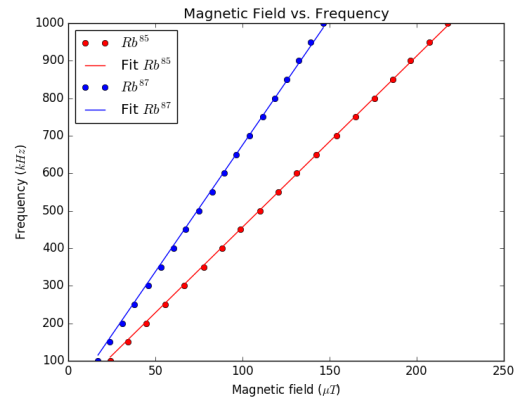


Figure 21: Frequency as a function of magnetic field.

(ii).a Zero field transition:

In the theory section we talked about the zero field transition and for the experiment we had to find this transition so as to be able to calibrate our measured magnetic field values so that there was no outside field interferences. A screenshot was taken of the zero field transition.

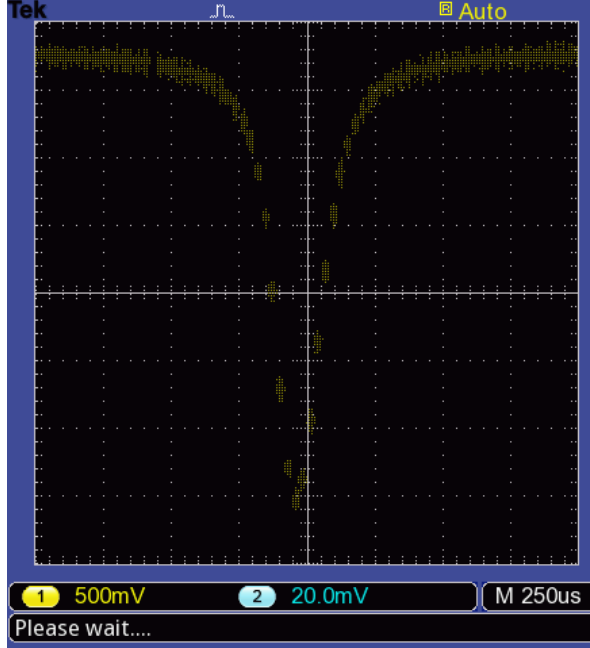


Figure 22: Zero field transition taken during part ii of the experiment in XY mode of the oscilloscope.

What we found was that the zero field transition had to be found by changing both the fields in the horizontal and vertical components. The vertical field was found to be  $51.2 \pm 0.3 \mu\text{T}$ . The horizontal was found to be  $10.1 \pm 0.1 \mu\text{T}$  when assuming the error in the voltmeter readings to be 0.002 V. We set the temperature to be  $50^\circ\text{C}$ .

(ii).b Measurement of  $g_F$  factors and nuclear spins:

In this section we wanted to find the  $g_F$  factors that we defined in equation 10 along with the nuclear spin (I). The method that we used to do this was by using an RF signal we varied the signal from 100 kHz up to 1 GHz in intervals of 50 kHz and measured the voltage on the coils at the moment that the rubidium atoms underwent the transition. The first transition at the resonance condition was taken as a screenshot from the oscilloscope and shown below.

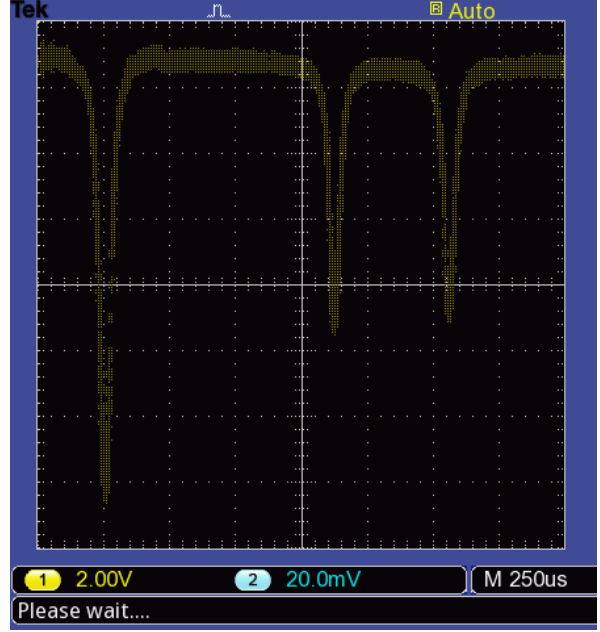


Figure 23: Screenshot of the first resonance condition at low fields at a frequency value of 100 kHz.

Data was taken at each frequency value and the values of the sweep field and horizontal field voltages, current and magnetic field were calculated along with the total field value. The data is shown on the table on the next page.

Rb <sup>85</sup>							
	Sweep field coil			Horizontal field coil			Combined
Frequency (kHz)	Voltage (V)	Current (A)	Field ( $\mu T$ )	Voltage (V)	Current (A)	Field ( $\mu T$ )	Field ( $\mu T$ )
100.0	0.5134	0.5134	30.9824	0.00184	0.0037	3.2272	24.0712
150.0	0.685	0.685	41.338	0.00184	0.0037	3.2272	34.4268
200.0	0.8575	0.8575	51.7479	0.00184	0.0037	3.2272	44.8368
250.0	0.7743	0.7743	46.727	0.0108	0.0216	18.9425	55.5311
300.0	0.579	0.579	34.9411	0.0239	0.0478	41.919	66.7218
350.0	0.5596	0.5596	33.7704	0.0308	0.0616	54.0212	77.6532
400.0	0.7333	0.7333	44.2527	0.0308	0.0616	54.0212	88.1356
450.0	0.9069	0.9069	54.7291	0.0308	0.0616	54.0212	98.6119
500.0	0.7126	0.7126	43.0036	0.044	0.088	77.1731	110.0383
550.0	0.7828	0.7828	47.2399	0.0477	0.0954	83.6627	120.7643
600.0	0.933	0.933	56.3041	0.0485	0.097	85.0658	131.2316
650.0	0.7178	0.7178	43.3174	0.0623	0.1246	109.2701	142.4491
700.0	0.4578	0.4578	27.627	0.0778	0.1556	136.4561	153.9448
750.0	0.446	0.446	26.9149	0.0844	0.1688	148.0321	164.8087
800.0	0.4736	0.4736	28.5805	0.0897	0.1794	157.3279	175.7701
850.0	0.6453	0.6453	38.9422	0.0897	0.1794	157.3279	186.1318
900.0	0.8175	0.8175	49.334	0.0897	0.1794	157.3279	196.5236
950.0	0.8299	0.8299	50.0823	0.0954	0.1908	167.3254	207.2693
1000.0	0.9125	0.9125	55.067	0.0986	0.1972	172.938	217.8666

Table 6: Data taken and calculated from known values. The Voltage columns and the frequency columns are from data that was taken.

Rb <sup>87</sup>							
	Sweep field coil			Horizontal field coil			Combined
Frequency (kHz)	Voltage (V)	Current (A)	Field ( $\mu T$ )	Voltage (V)	Current (A)	Field ( $\mu T$ )	Field ( $\mu T$ )
100.0	0.3974	0.3974	23.9821	0.00184	0.0037	3.2272	17.0709
150.0	0.511	0.511	30.8375	0.00184	0.0037	3.2272	23.9264
200.0	0.6265	0.6265	37.8076	0.00184	0.0037	3.2272	30.8965
250.0	0.4843	0.4843	29.2262	0.0108	0.0216	18.9425	38.0304
300.0	0.2327	0.2327	14.0428	0.0239	0.0478	41.919	45.8235
350.0	0.1553	0.1553	9.372	0.0308	0.0616	54.0212	53.2548
400.0	0.2728	0.2728	16.4628	0.0308	0.0616	54.0212	60.3456
450.0	0.388	0.388	23.4148	0.0308	0.0616	54.0212	67.2976
500.0	0.1347	0.1347	8.1288	0.044	0.088	77.1731	75.1636
550.0	0.1486	0.1486	8.9676	0.0477	0.0954	83.6627	82.4919
600.0	0.2413	0.2413	14.5618	0.0485	0.097	85.0658	89.4893
650.0	0.3565	0.3565	21.5138	0.0485	0.097	85.0658	96.4413
700.0	0.2671	0.2671	16.1188	0.0558	0.1116	97.8696	103.85
750.0	0.1556	0.1556	9.3901	0.064	0.128	112.2518	111.5035
800.0	0.2695	0.2695	16.2636	0.064	0.128	112.2518	118.3771
850.0	0.2678	0.2678	16.161	0.068	0.136	119.2676	125.2902
900.0	0.384	0.384	23.1734	0.068	0.136	119.2676	132.3026
950.0	0.4989	0.4989	30.1073	0.068	0.136	119.2676	139.2365
1000.0	0.5807	0.5807	35.0437	0.0693	0.1386	121.5477	146.4531

Table 7: Data taken and calculated from known values. The Voltage columns and the frequency columns are from data that was taken.

The data from tables 5 and 6 is included under the frequency and the voltage columns for the the sweep field and the horizontal field coil. The currents were calculated from Ohm's law where the sweep field had a  $1\ \Omega$  resistor and the horizontal field had a  $0.5\ \Omega$  resistor. The fields were calculated using equation 21. The combined field was found by adding the magnetic fields from both coils and then subtracting the value of the zero field magnetic field value.

A plot of the frequency as a function of the combined magnetic field is shown on figure 21. Using equation 11 it is easy to see the linear relationship between the slope and the  $g_F$  factor which when the equation is solved for the value we get values of  $0.3260 \pm 0.0005$  and  $0.482 \pm 0.001$  for  $Rb^{85}$  and  $Rb^{87}$  respectively. By then having the  $g_F$  factor we can solve for the nuclear angular momentum (I) by rewriting equation 10 for I and we get the algebraic expression.

$$0 = 2I^2 g_F + 2I(g_F + J[2g_F - g_J]) - 2J(J+1)(g_J - g_F) \quad (22)$$

Where,  $g_F$  has just been calculated,  $g_J$  is the Lande g-factor, J is equal to  $1/2$ . Equation 22 takes the form of a quadratic and can be solved for I and when taking the positive roots the values that are gotten for the nuclear spin are 2.571 and 1.576 for  $Rb^{85}$  and  $Rb^{87}$  respectively.

### (iii) Quadratic Zeeman Effect

For this part of the experiment we studied the Zeeman resonances of both isotopes. We will study the region in which the energy level splitting is no longer linear nor equally spaced and there will be a total of 2F resonances. The relative intensities of the signals depend on the pumping conditions.

#### (iii).a $Rb^{87}$ quadratic Zeeman effect

For this part of the experiment we used the following settings to view the quadratic Zeeman effect at low RF power for the  $Rb^{87}$ .

Detector amplifier gain = 20

Mutiplier = 20

$\nu = 5.95\ \text{MHz}$

Time constant = 100 ms

RF amplifier gain = 3

Sweep time = 50 s

Horizontal Field current = 0.9872 A

RF amplitude = 1 V

The data that was collected is the following.

Peak	Amplitude (500 mV)	Voltage (V)
1	1.2	0.1095
2	1.6	0.1337
3	2.5	0.1580
4	3.4	0.1821

Table 8: Data taken for low RF power quadratic Zeeman effect

The plot of the data is shown on figure 24 where the Voltage column is the voltage measured for the sweep field coil. To get the magnetic field we added the magnetic fields of the sweep and the horizontal magnetic coils and subtracted the zero field value.

The screenshot of the data that was taken on the oscilloscope is shown below.

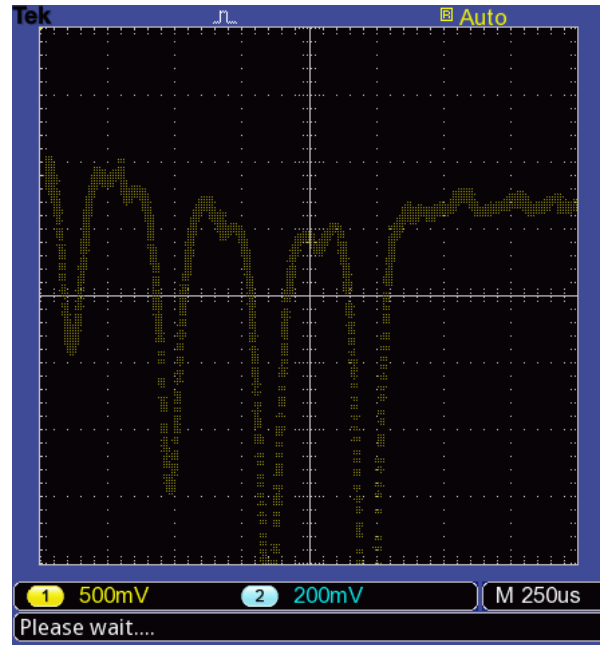


Figure 28: Quadratic Zeeman effect of  $Rb^{87}$  at low RF power

Now we will consider the double quadratic Zeeman effect. For this we used the settings.

Detector amplifier gain = 20

Mutiplier = 20

$\nu = 5.95\ \text{MHz}$

Time constant = 100 ms

RF amplifier gain = 3

Sweep time = 50 s

Horizontal Field current = 0.9872 A

RF amplitude = 2.5 V

The data collected was the following.



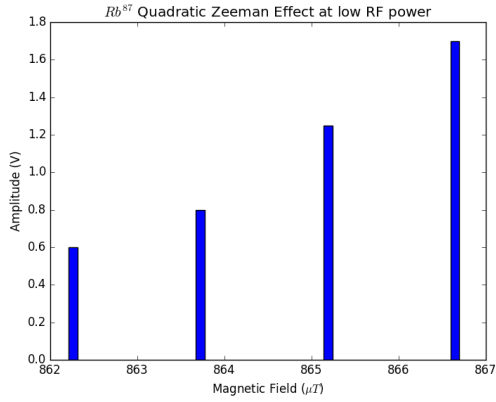


Figure 24:  $Rb^{87}$  quadratic zeeman effect at low RF power

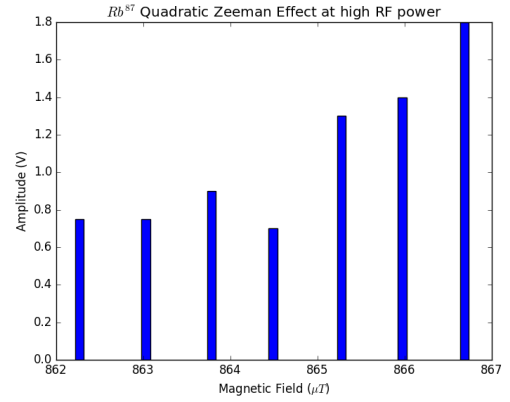


Figure 25:  $Rb^{87}$  double quadratic zeeman effect at high RF power

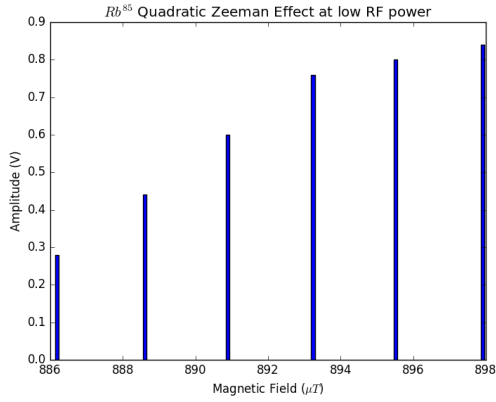


Figure 26:  $Rb^{85}$  quadratic zeeman effect at low RF power

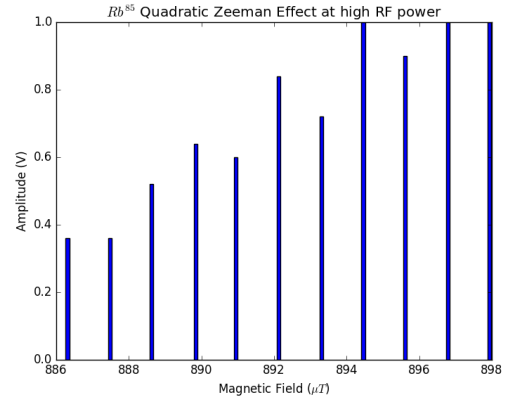


Figure 27:  $Rb^{85}$  double quadratic zeeman effect at high RF power

Peak	Amplitude (500 mV)	Voltage (V)
1	1.5	0.1096
2	1.5	0.1222
3	1.8	0.1347
4	1.4	0.1464
5	2.6	0.1594
6	2.8	0.1710
7	3.6	0.1828

Table 9: *Data taken for high RF power double quadratic Zeeman effect*

The plot of the data is shown on figure 25. Where, the same explanation as before still applies. The screenshot of the double quantum transition is the following.

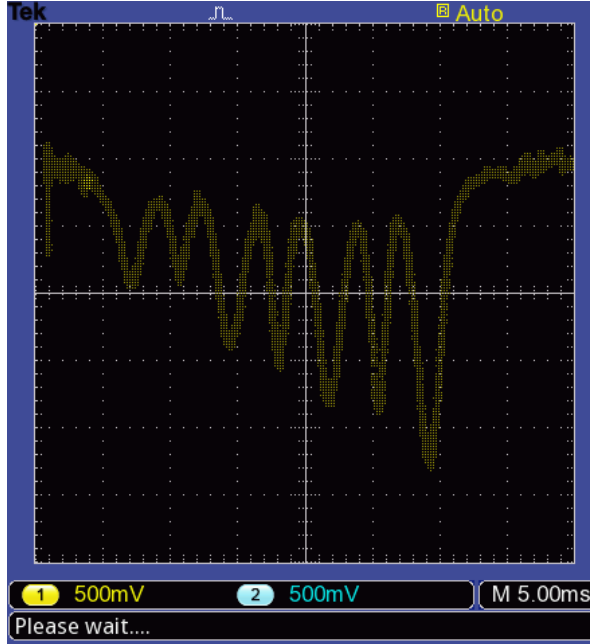


Figure 29: *Quadratic Zeeman effect of  $Rb^{87}$  at high RF power*

### (iii).b $Rb^{85}$ quadratic Zeeman effect

Now we consider the quadratic Zeeman effect of  $Rb^{85}$ . The settings are as follows.

Detector amplifier gain = 20

Mutiplier = 10

$\nu = 4.1$  MHz

Time constant = 100 ms

RF amplifier gain = 3

Sweep time = 50 s

Horizontal Field current = 0.9872 A

RF amplitude = 1.0 V

The data that was collected was the following.

Peak	Amplitude (200 mV)	Voltage (V)
1	1.4	0.5060
2	2.2	0.5460
3	3.0	0.5839
4	3.8	0.6228
5	4.0	0.6604
6	4.2	0.7002

Table 10: *Data taken for low RF power quadratic Zeeman effect*

The plot of the data is shown on figure 26. The screenshot of the oscilloscope data is the following.

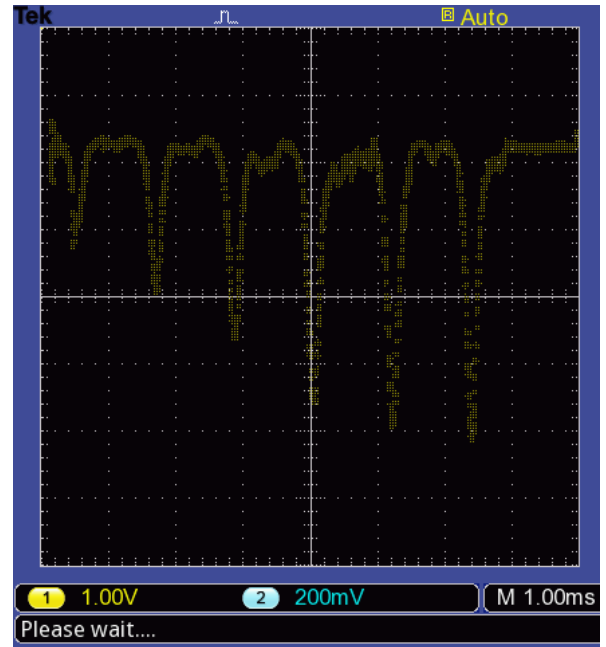


Figure 30: *Quadratic Zeeman effect of  $Rb^{85}$  at low RF power*

We will now consider the quadratic zeeman effect at high RF power.

The settings used were the following.

Detector amplifier gain = 20

Mutiplier = 10

$\nu = 4.1$  MHz

Time constant = 100 ms

RF amplifier gain = 3

Sweep time = 50 s

Horizontal Field current = 0.9872 A

RF amplitude = 2.5 V

With the data collected being the following.

Peak	Amplitude (200 mV)	Voltage (V)
1	1.8	0.5080
2	1.8	0.5273
3	2.6	0.5463
4	3.2	0.5664
5	3.0	0.5848
6	4.2	0.6045
7	3.6	0.6239
8	5.0	0.6430
9	4.5	0.6620
10	5.0	0.6817
11	5.0	0.7005

Table 11: *Data taken for low RF power quadratic Zeeman effect*

The plot of the data is shown on figure 27. The screenshot of the oscilloscope data is the following.

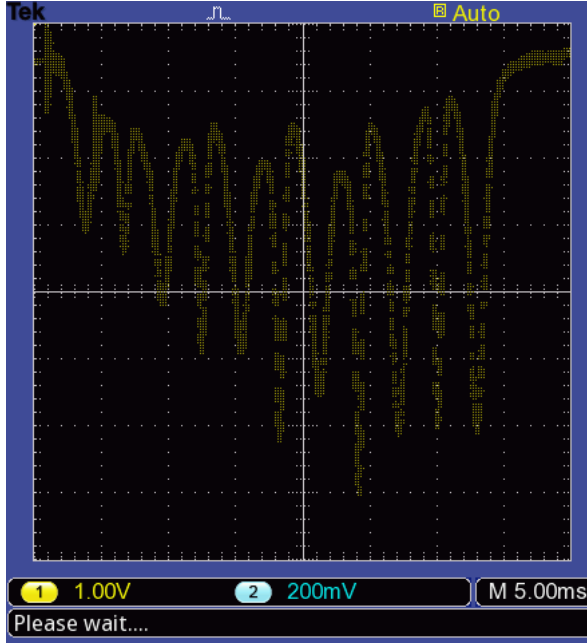


Figure 31: *Quadratic Zeeman effect of  $Rb^{85}$  at high RF power*

#### (iv) Transient effects

For this part of the experiment we wanted to see what would happen where we to turn the RF magnetic field on and off quickly. Making pulses of RF magnetic fields. We first set the following parameters.

Detector amplifier gain = 1  
Multiplier = 1  
 $\nu = 100$  kHz

Time constant = min.  
RF amplifier gain = 8  
Sweep time = 50 s  
Horizontal Field current = 3.68 mA  
RF amplitude = 1.0 V

We found that by plotting the incoming channels against time on the oscilloscope we got the following figure.

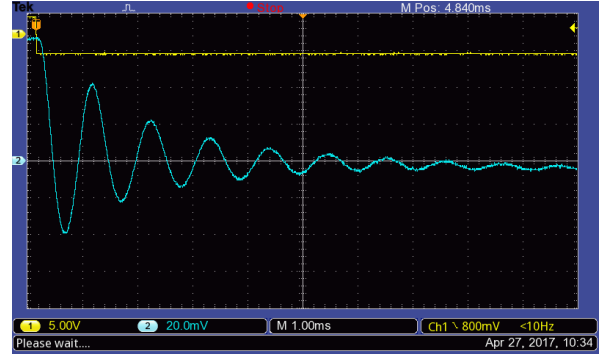


Figure 33: *Oscillations of the light intensity at 100 kHz and RF amplitude of 1.0 V.*

When we have the RF oscillate on and off at a frequency of 5 Hz we find that we get that picture when the RF is suddenly turned off. We did this for both of the isotopes of rubidium from RF amplitudes of 1.00 V to 4.00 V. When we looked for all the maxima in the figure and found the avreage period of oscillations we found that we got the following periods of oscillations.

RF Amplitude (V)	$Rb^{85}$ Period ( $\mu s$ )	$Rb^{87}$ Period ( $\mu s$ )
1.00	1067.2	723.0
1.20	861.6	606.7
1.40	757.0	508.8
1.60	659.2	442.0
1.80	586.0	390.0
2.00	534.4	352.8
2.20	501.3	334.4
2.40	457.7	304.8
2.60	421.7	279.3
2.80	394.5	264.7
3.00	377.5	252.7
3.20	367.0	246.7
3.40	360.5	240.7
3.60	354.0	238.0
3.80	350.9	233.3
4.00	347.5	232.7

Table 12: Data that was used for figure 32  
The data for the RF amplitude on table 12 was

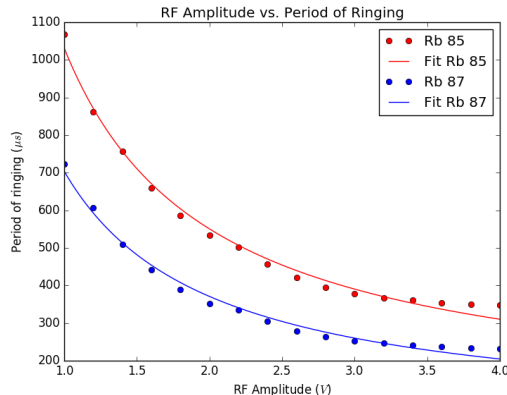


Figure 32: Plot of the period of ringing in light intensity as a function of RF amplitude.

taken directly from the RF signal generator. The second column was gotten by reading through the data on each of the generated oscillation signals and finding the respective maxima. This was done by exporting the screenshot of the oscilloscope to save all of the data files which includes two .CSV files for each of the signals. By using this we can get a much better estimate for the period as we do not have to manually do it and introduce human error due to inability to read difference in pixels. By fitting the plots to an equation that reads.

$$Y = \frac{A}{x} + B \quad (23)$$

Where, x is the RF amplitude, Y the period of the ringing and the A, B parameters were calculated in Python with the curve fitting function to be.

	A	B
$Rb^{85}$	$960.0 \pm 20.0$	$70.0 \pm 10.0$
$Rb^{87}$	$670.0 \pm 20.0$	$38.0 \pm 9.0$

Table 13: Fit parameters to equation 23

Having calculated these values we were then able to find the ratio of the period of the ringing by dividing the A values. We found this value to be  $1.44 \pm 0.05$ .

When we compare this value to the expected value of 1.50 we believe to be sufficiently close to be able to take this value.

## References

- [1] Bloom, A L (1960). Optical Pumping. *Scientific American* October, 72.
- [2] Benumof, R (1965). Optical Pumping Theory and Experiments. *American Journal of Physics* 33, 151.

[3] UB 2015 Lab Manual. Optical Pumping.

[4] Griffiths, D J (2005). Introduction to Quantum Mechanics. Upper Saddle river, New Jersey: Pearson Prentice Hall.